Published in final edited form as:
J Biol Chem. 1991 July 25; 266(21): 13958–13963.

A Long Helix from the Central Region of Smooth Muscle Caldesmon*

C.-L. Albert Wang‡,§, **Joseph M. Chalovich**¶, **Philip Graceffa**‡, **Renné C. Lu**‡,||, **Katsuhide Mabuchi**‡, and **Walter F. Stafford**‡,||

‡ *From the Department of Muscle Research, Boston Biomedical Research Institute, Boston, Massachusetts 02114, the*

|| *Department of Neurology, Harvard Medical School, Boston, Massachusetts 02115, and the*

¶ *Department of Biochemistry, East Carolina University Medical School, Greenville, North Carolina 27858*

Abstract

The central region of smooth muscle caldesmon is predicted to form α-helices on the basis of its primary structure. We have isolated a fragment (CT54) that contains this region. The hydrodynamic properties and the electron microscopic images suggest that CT54 is an elongated (35 nm), monomeric molecule. The circular dichroic spectrum yields an overall α-helical content of 55–58%. These results are consistent with the model that the middle portion of CT54 forms a long stretch of single-stranded α-helix. Such a structure, if it in fact exists, is thought to be stabilized by numerous salt bridges between charged residues at positions *i* and *i*+4. The structural characteristics of this fragment not only represent an unusual protein configuration but also provide information about the functional role of caldesmon in smooth muscle contraction.

Both smooth muscle and non-muscle cells contain a major heat-stable, actin-binding protein, caldesmon (1, for reviews, see Refs. 2,3). Although the exact physiological role of caldesmon remains uncertain, its inhibition of actomyosin-activated ATP hydrolysis *in vitro* (4–7), its ability to respond to changes of the calcium concentration via interactions with calmodulin (4–6), and its binding to myosin (8,9) have prompted much speculation that this thin filament-associated protein may be involved in some auxiliary mechanism for regulation (10–12). On the basis of its predicted secondary structure (13,14) and recent electron microscopic images (15), the molecule of smooth muscle caldesmon can be roughly divided into three parts: the N-terminal portion (residues 1–249),[1] the middle portion (residues 250–396), and the C-terminal portion (residues 397–756). The non-muscle form, however, has only the two terminal portions, with the middle part found in smooth muscle caldesmon missing (3,16–18). The muscle form of caldesmon is better characterized than the non-muscle isoform both structurally and functionally. The C-terminal portion contains most of the functional domains, *viz.* regions for actin binding (19–22), calmodulin binding (19,20,22–25), and ATPase inhibition (19,23); the N-terminal portion contains the myosin-binding site (26–28) and a putative, secondary,

*This work was supported by National Institutes of Health Grants HL41411 (to C. L. A. W.), AR35216 (to J. M. C.), AR30917 (to P. G.), AR28401, and RR03370 (to R. C. L.) and American Heart Association Grant-in-aid 901345 (to C. L. A. W.).

§ Established Investigator of the American Heart Association. To whom all correspondence should be addressed: Dept. of Muscle Research, Boston Biomedical Research Institute, 20 Staniford St., Boston, MA 02114..

[1]To this date, there are two non-identical cDNA clones from the chicken gizzard library that have been identified and sequenced. One isoform (771 residues, Ref. 14) is 15 residues longer than the other (756 residues, Ref. 13). The difference (AAEERERAKAEEERK) occurs in the middle part of the molecule, where the longer isoform contains an extra repeating unit (see "Results and Discussion"). The degree of precision in our amino acid composition analysis results (Table I) does not allow us to differentiate between the two isoforms, although the molecular weight is more consistent with the smaller isoform. For the sake of discussion, we assume our CT54 is from the 756-residue isoform and use the numbering system of this smaller form unless indicated otherwise.

calmodulin-binding site (25,29). No known function has yet been assigned to the middle portion, although the amino acid sequence suggests that it has a tendency to form α-helical structures (13,14). Here we report the isolation of a fragment (CT54)[2] that has an apparent molecular weight from sodium dodecyl sulfate-gel electrophoresis of 54,000 and contains the middle part of the smooth muscle caldesmon molecule. We present evidence for the existence of a long α-helical stretch in this fragment. The unusual length and stability of this rod-like structure may serve as a spacer between the myosin-binding site and the actin-binding site.

MATERIALS AND METHODS

Purification of Caldesmon and CT54

Turkey gizzard caldesmon was purified as previously described (30). Purified caldesmon (5 mg/ml) in 0.1 m NaCl, 10 mm imidazole, pH 7.0, 1 mm dithiothreitol (buffer A) was cleaved with α-chymotrypsin (Worthington) at 1:700 ratio (chymotrypsin to caldesmon, by weight) at 25 °C for 5 min. After termination of the reaction with phenylmethanesulfonyl fluoride, the mixture was loaded onto a 2.5 × 20-cm column of Affi-Gel Blue (100–200 mesh, Bio-Rad) equilibrated with the same buffer. The crude CT54, which did not cosediment with F-actin, was eluted with 250 mm NaCl, 10 mm Tris-HCl, pH 8.0, 1 mm dithiothreitol, and was further purified on an ACA 54 column (1.5 × 90-cm, Spectrum) equilibrated with buffer A. After concentration on an Amicon Filtration apparatus using a YM-2 membrane, the sample was dialyzed against 50 mm NaCl, 10 mm Tris-MES, pH 7.0. The sample was then chromatographed on a Waters HPLC using a Pharmacia LKB Biotechnology Inc. Mono Q column with an exponential gradient to 500 mm NaCl. The major peak was concentrated and chromatographed on the same column using a linear gradient on NaCl from 185 to 500 mm (Fig. 1, *A* and *B*).

Ultracentrifugation Studies

Sedimentation equilibrium runs were performed as described previously (31). CT54 (0.5 mg/ml) was centrifuged at 20,000 rpm for 72 h. A value of 0.723 cm^3/g for the partial specific volume of CT54 at 4 °C was calculated from the amino acid composition (Table I). A value of 0.612 g of H_2O/g of protein for the hydration was calculated using the values for the individual amino acids from Kuntz and Kauzman (32). Sedimentation velocity runs were carried out as described previously at 20 °C (31).

Circular Dichroism Measurements

CD spectra were measured in a 1-cm path length cell on an Aviv Associates (Lakewood, NJ) model 60 DS spectropolarimeter containing a Hewlett-Packard 89100A temperature controller. CT54 spectra were corrected by subtracting buffer spectra, and the observed ellipticity was converted to mean residue weight ellipticity, $[\theta]$ (degree-cm^2/dmol). The helical contents were calculated from $[\theta]_{208\ nm}$ or by curve fitting to basis spectra according to Greenfield and Fasman (33). Temperature-dependent CD measurements were carried out at 1.0 °C intervals as described previously (34).

Determination of Protein Concentration

The concentration of CT54 was determined by three independent methods: (i) Lowry assay using rabbit skeletal muscle tropomyosin as a standard (35); (ii) amino acid composition analysis (see below for details); and (iii) refractive index measurements by ultracentrifugation (see Ref. 31 for details). All three methods yielded values which agreed within a standard

[2]The abbreviations used are: CT54, the chymotryptic fragment of caldesmon having an apparent molecular weight of 54,000; MES, 2-(*N*-morpholino)ethanesulfonic acid; HPLC, high performance liquid chromatography.

deviation of 3–5%. Concentrations estimated on the basis of the molar extinction coefficient of 5600 at 280 nm for tryptophan (36) agree reasonably well with values obtained from the other three methods.

Electron Microscopic Studies

CT54 was examined by the minimum angle vertical rotary shadowing technique (37) on a Philips EM 300 electron microscope at 60 kV. Other experimental details were as previously described (15).

Amino Acid Analysis

N-terminal amino acid sequence analyses were performed on an Applied Biosystems Sequencer (model 477A) with an on-line phenylthiohydantion analyzer (model 120A). To determine the amino acid composition, the fragment was hydrolyzed in 6 m HCl for 20 h at 110 °C under vacuum, and the analyses were performed on a Beckman High Performance Amino Acid Analyzer (model 7300).

RESULTS AND DISCUSSION

The 54-kDa caldesmon fragment (CT54) exhibits remarkable resistance to chymotryptic cleavage (Fig. 1*C*). This fragment, purified by high performance liquid chromatography after digestion with chymotrypsin (Fig. 1*A* and *B*), does not bind to actin, although it can be retained on a myosin-Sepharose column under low salt (35 mm) conditions.[3] CT54 migrates on polyacrylamide gel electrophoresis in the presence of $NaDodSO_4$ with an apparent molecular weight of 54,000, although the actual molecular weight is about 33,000 on the basis of sedimentation equilibrium experiments (Fig. 2). Such a discrepancy between the apparent and true molecular weights has also been reported for the parent molecule (31) and was attributed to its poor ability to bind the detergent owing to a high content of acidic residues (38,39). The amino acid composition analysis of CT54 (Table I) shows 40% Glx + Asx, consistent with a high acidic residue content. N-terminal sequence analysis reveals some heterogeneity in this CT54 preparation: the main component (>75%) begins at Gln^{166}, resulting from cleavages at Tyr^{165}, whereas the minor component (<25%) begins at Arg^{171}, resulting from cleavages at Trp^{170}.

The results of our amino acid sequence and composition analyses indicate that CT54 is a 285-residue peptide extending from Gln^{166} to Trp^{450}, with a calculated molecular weight of 33,060, consistent with the hydrodynamic measurements (see above). The fact that the majority of the fragment contains an internal tryptophan residue (Trp^{170}) suggests that this residue is situated in a somewhat protected environment. There are 10 Val, 10 Leu, and 1 Ile in CT54; these residues, normally susceptible to chymotrptic cleavages, must also be protected in order to account for their insensitivity toward the enzyme.

Thus, CT54 covers part of the N-terminal portion and the entire middle portion of caldesmon and amounts to about one-third of the whole molecule. Notably, this central region contains at least nine repeats of a 12-residue unit, KAEEEK(or R)KAAEEK (Fig. 3) and has been predicted by a number of secondary structure algorithms to have a high tendency to form α-helical structures (13,14). In particular, the 147 residues between 250–396 are predicted to be in an uninterrupted string of α-helical structure with little or no tendency to form β-sheet or random coil (Fig. 4). Analysis of the circular dichroism spectrum of CT54 (Fig. 5*A*) gives 55 ± 2% α-helical content from the ellipticity at 208 nm, and 58 ± 2% α-helical content with the remainder

[3]While CT54 may bind to myosin, the major portion of the myosin-binding region is located in the N-terminal chymotryptic fragment of caldesmon.

being random coil from curve fitting to basis spectra (33). This indicates that about 160 residues of CT54 are in an α-helical structure. It is interesting to note that non-muscle (liver) caldesmon lacks the central repeating region, 232 amino acid residues from Val^{200} being deleted, and has a lower helical content (Table II). The difference in the α-helical content between the intact muscle caldesmon (40) and the non-muscle isoform (see Table II) corresponds to ~140 α-helical residues in this "difference peptide." These results are consistent with the idea that the central repeating region in smooth muscle caldesmon is nearly 100% helical.

The α-helical structure of CT54 is highly stable, since it is rather insensitive to changes in ionic strength and pH and unfolds at a relatively high temperature. The CD spectrum of CT54 at 20 °C remained essentially unchanged upon varying [NaCl] from 0 to 1.0 m at pH 7, and over a wide range of pH, from 2 to 9.5 in 50 mm NaCl (Fig. 5*B*). There was about a 10% drop in the α-helical content upon further increase in pH to 11 (Fig. 5*B*). The extraordinary stability against both salt concentration and pH is noteworthy, and may be attributable to the intra-helical salt bridges (see below).

CT54 undergoes a gradual thermal unfolding upon increasing the temperature from 5 to 90 ° C at pH 7 (Fig. 5*B*). The ellipticity of the fragment decreases gradually up to 40 °C and then, somewhat more steeply, to 80 °C with an overall midpoint temperature ($T_{1/2}$) at about 50 °C (Fig. 5*B*). While the apparent $T_{1/2}$ remains unchanged at pH 9.5 and only slightly decreases at pH 2, it is considerably lower at pH 11 (Fig. 5*B*). These properties are similar to those of an 80-residue, highly α-helical (80%) fragment (CB2) of troponin T (41) and of certain synthetic peptides (see below), which also unfold over a relatively wide temperature range. In contrast to the much sharper thermal transitions exhibited by α-helical coiled-coils, *e.g*. tropomyosin (35) and myosin rod (42), the observed gradual decrease in ellipticity of CT54 may result from a loss of less cooperative interactions that are responsible for maintaining the structure. This behavior could reflect the unfolding of a highly stabilized helix, either from the ends inward, or randomly and segmentally along the entire helix.

The CT54 fragment in solution is highly asymmetric as indicated by sedimentation velocity experiments, which yield a sedimentation coefficient of 1.44 S and an axial ratio of 24 with the length and diameter of 35.6 nm and 1.46 nm, respectively, assuming a simple unhydrated prolate ellipsoid. This model should be compared to the electron microscopic results (see below). The hydrodynamic properties of a string-of-beads model were also calculated using the program GENTRA developed by Garcia de la Torre (43). The observed molecular weight and sedimentation coefficient can be best modeled with a rod-shaped string of 38 beads that has a diameter of 1.00 nm and an overall length of 38.0 nm. Other models such as dumbbell-shaped string of beads do not yield good fits, suggesting that CT54 is a uniformly elongated molecule with little features at both ends, consistent with the electron microscopic observations (see below).

The molecular dimension was also studied by electron microscopic visualization of the fragment using rotary shadowing (Fig. 6), which reveals a rod-like image, similar to, although shorter than, the intact gizzard caldesmon (10). The thickness appears less than that of the myosin rod and tropomyosin, confirming that CT54 is not a coiled coil. The average contour length is about 35 nm (Fig. 6, *inset*), in good agreement with the unhydrated dimension calculated from the hydrodynamic parameters. As there is no evidence for dimerization (*cf*. ultracentrifugation results, see Fig. 2), the observed molecular length is that of a monomer. This length is consistent with an extended helical stretch of 157 residues (*i.e*. 55% of the 285 residues of CT54) that spans a length of 24.2 nm, with additional length due to the remaining, non-helical 128 residues. The observed length would be too long for a folded structure, an anti-parallel hairpin, for example, since an 80-residue helix spans only 12.3 nm. It is noteworthy that the difference in length between unhydrated muscle (31) and non-muscle (3) caldesmons,

as determined by hydrodynamic measurements, is about 21 nm (±3 nm). This value corresponds to a minimum length of the difference peptide (see above and Table II) that contains the central repeating sequence of muscle caldesmon and constitutes a subdomain (232 compared to 285 residues) of CT54. This difference is consistent with the observed dimension of CT54.

The possibility of shorter α-helical segments interspersed with random coil or turns was also considered. But this seems unlikely because (i) there are no apparent breaks in the central repeating region, judging from the amino acid sequence; (ii) discontinuous helical stretches would disrupt salt bridges and may not be energetically favored (see below); and (iii) foldings or bends in the helical stretch would tend to further shorten the length of the repeating region, and thus would be inconsistent with the electron microscopic and hydrodynamic observations. We therefore propose that the middle part of CT54 (from about Lys^{250} to Ala^{396}, Fig. 3) exists as a long, continuous, single α-helix, while the rest of the fragment is neither α-helical nor in β-sheet. The visability of a single helical rod under the electron microscope is quite remarkable, and is most likely due to its abundant long side-chains.

Single helical structures have been proposed for many synthetic peptides, such as poly-l-lysine, poly-l-glutamate, and $(Lys\text{-}Glu)_n$ copolymers. Similar structures in naturally occurring proteins, such as troponin T (41), troponin C (44,45), calmodulin (46), and certain antifreeze proteins (47), have also been described. The length of the helical stretch found in these proteins, however, is considerably smaller compared to the one observed in CT54. It has been suggested that in aqueous solution single α-helices are stabilized by intra-helical salt bridges between residues *i* and *i*+4 (48–52). Indeed the stability of α-helices held by (*i*+4)-type salt bridges is quite remarkable. A synthetic 17-mer, (*i*+4)Glu,Lys, for example, unfolds over a temperature range of 50–60 degrees; this peptide also remains stable at both pH extremes (pH 2 and 13), and only loses 16% of its helical content when the salt concentration is raised from 0.01 to 1.0 m (49). The (i+3)Glu,Lys peptide, on the other hand, has a much lower helical content under the same conditions and melts at a lower temperature (49,52). There are a total of 86 Glu, 56 Lys, and 21 Arg in the sequence of CT54, most of which are able to interact with a side chain of an opposite charge at *i*+4 positions (Fig. 7). The 12 residues in a basic repeating unit contain four pairs of salt bridges between the *i*th and the *i*+4th residues, giving rise to a total of at least 36 possible pairs of charge interactions between Glu and Lys (or Arg). Such a high density of these charge interactions may thus stabilize the long helix over a wide range of salt concentration and pH. For reasons not well understood, Glu, as the negative charge in the salt bridges, provides additional helical stability at pH extremes (from pH 1 to 13) when compared to Asp (48,49,51,52). This may further explain the observation that the CD spectrum is not sensitive to pH changes, since all negatively charged residues in the helical region of CT54 are Glus.

It is also noteworthy that, although (*i*+4)Glu,Lys exhibits a higher helical content than does the isopeptide (*i*+4)Lys,Glu in low salt (0.01 m NaCl), the latter is better able to maintain the secondary structure than the former in high (1.0 m) salt concentration (see Table 1 in Ref. 52). This could be attributed to the effect of the macrodipole moment (53), which is presumably stabilized by the formation of Glu-to-Lys salt bridges but not by the salt bridges of reversed direction (52). Almost all of the salt bridges found in the helical region of CT54 are from Lys (or Arg) to Glu. This may be relevant to the observed stability against the salt concentration. In view of the recent work by Åqvist *et al.* (54), however, it remains unsettled whether the helix macrodipole plays any significant role in electrostatic stabilization. Nevertheless, it is interesting to note that in CT54 there are several clusters of negative charges in the N-terminal, presumably non-helical, region (residues 166–240), giving a net formal charge of −13. Similarly, there is a net formal charge of +1 in the C-terminal non-helical region (residues 400–450). It is possible that the helical dipole moment is already stabilized by these electrostatic

interactions, so that it no longer relies on the directionality of the intra-helical salt bridges. The inter-relationships between the helical stability, the terminal charges, and the direction of salt bridges may deserve more detailed studies.

Finally, the tightly associated side chains of the charged residues may be prevented from interacting with other residues. This idea is consistent with the observations in both ultracentrifugation and electron microscopic studies that there is very little side-by-side or other interactions between the fragments. All the residues involved in the intra-helical salt bridges have long side chains (Glu and Lys); this may provide the rigidity that is needed to allow their observation under the shadowing conditions. The regularly spaced (Fig. 7), protruding salt bridges may also protect the hydrophobic residues against proteolysis. It is interesting to note that there are 33 Ala residues in the central repeating region, being the only major uncharged amino acid in the sequence. This further supports the salt bridge model, since the small methyl group of Ala would not interfere with the interactions between the charged side chains (49).

There are several irregularities found in the central repeating sequence; the existence of these odd residues can be readily understood once the salt bridge model is adopted. For example, there are 3 Glus in the repeating sequence Lys-Ala-Glu-Glu-Glu-Lys (or Arg); since the middle one in the triplet is not used in salt-bridging, it may be altered without affecting the stability of the helix within limits. This may explain the presence of Lys^{349} in the seventh repeating unit (residues 346–357, see Fig. 3). Similarly, in the eighth unit there is an 11-residue insert after Lys^{372} but now the pattern is disrupted so that it ends with a Lys (Lys^{383}), it is followed by a 2-Glu sequence (Lys-Lys-Met-Glu-Glu-Lys) in which Met^{386} assumes a position in which a Glu would otherwise be. Charge interactions between *i* and *i*+4 positions can also be found in regions outside the repeating sequences, but they are rare. It is not clear whether these putative salt bridges would stabilize other α-helical structures in the two end-domains.

Smooth muscle caldesmon inhibits actin-activated ATP hydrolysis by myosin but under some conditions it actually results in an increase in the amount of myosin associated with actin (7). This behavior has been explained by the observation that caldesmon has two functions (8). (i) Caldesmon can bind to actin and inhibit the binding of myosin resulting in a decreased rate of ATP hydrolysis. (ii) Caldesmon also can bind to myosin and thereby form a bridge between actin and myosin. The actin-binding region of caldesmon is in the C-terminal region (19–22), while the myosin binding region is in the N-terminal region (26–28). Interestingly, the binding of caldesmon to myosin is similar in strength to its binding to actin (55). A rod-like structure in caldesmon described here may serve as a spacer to separate these binding domains, or to enable the N-terminal end to reach myosin while the C-terminal end is anchored to actin. It should be noted that the non-muscle form of caldesmon does not contain such a central region (3,16–18), suggesting that a spacer may not be needed in the non-muscle system. Among other differences between the muscle and non-muscle systems, non-muscle myosin is not in the form of organized filaments, in contrast to that in the muscle system. The structural difference between the smooth muscle and the non-muscle forms of caldesmon may, therefore, be determined by their different functional roles.

Acknowledgements

We wish to thank Mr. Zheng Gong for his technical assistance. We also thank Dr. J. Gergely for critical reading of this manuscript.

References

1. Sobue K, Muramoto Y, Fujita M, Kakiuchi S. Proc Natl Acad Sci U S A 1981;78:5652–5655. [PubMed: 6946503]
2. Pritchard K, Moody CJ. Cell Calcium 1986;7:309–327. [PubMed: 3545485]

3. Stafford WF, Jancso A, Graceffa P. Arch Biochem Biophys 1990;281:66–69. [PubMed: 2383024]
4. Sobue K, Morimoto K, Inui M, Kanda K, Kakiuchi S. Biomed Res 1982;3:188–196.
5. Marston SB, Moody CJ, Smith CWJ. Biochem Soc Trans 1984;12:945–948. [PubMed: 6530043]
6. Ngai PK, Walsh MP. J Biol Chem 1984;259:13656–13659. [PubMed: 6150036]
7. Lash JA, Sellers JR, Hathaway DR. J Biol Chem 1986;261:16155–16160. [PubMed: 2946681]
8. Hemric ME, Chalovich JM. J Biol Chem 1988;263:1878–1885. [PubMed: 2962997]
9. Ikebe M, Reardon S. J Biol Chem 1988;263:3055–3058. [PubMed: 3257755]
10. Marston SB, Smith CWJ. J Muscle Res Cell Motil 1985;6:669–708. [PubMed: 3937845]
11. Chalovich JM. Cell Biophys 1988;12:73–85. [PubMed: 2453287]
12. Marston SB. J Muscle Res Cell Moltil 1989;10:97–100.
13. Bryan J, Imai M, Lee R, Moore P, Cook RG, Lin WG. J Biol Chem 1989;264:13873–13879. [PubMed: 2760048]
14. Hayashi K, Kanda K, Kimizuka F, Kato I, Sobue K. Biochem Biophys Res Commun 1989;164:503–511. [PubMed: 2803315]
15. Mabuchi K, Wang CLA. J Muscle Res Cell Motil 1991;12:145–151. [PubMed: 2061408]
16. Ball EH, Kovala T. Biochemistry 1988;27:6093–6098. [PubMed: 3191109]
17. Hayashi K, Fujio Y, Kato I, Sobue K. J Biol Chem 1991;266:355–361. [PubMed: 1824698]
18. Bryan J, Saavedra-Alanis V, Wang CLA, Wang LWC, Lu RC. J Muscle Res Cell Moltil 1990;11:434.
19. Szpacenko A, Dabrowska R. FEBS Lett 1986;202:182–186. [PubMed: 2941315]
20. Fujii T, Imai M, Rosenfeld GC, Bryan J. J Biol Chem 1987;262:2757–2763. [PubMed: 2434491]
21. Leszyk J, Mornet D, Audemard E, Collins JH. Biochem Biophys Res Commun 1989;160:1371–1378. [PubMed: 2730648]
22. Yazawa M, Yagi K, Sobue K. J Biochem (Tokyo) 1987;102:1065–1073. [PubMed: 3436963]
23. Bartegi A, Fattoum A, Derancourt J, Kassab R. J Biol Chem 1990;265:15231–15238. [PubMed: 2394719]
24. Takagi T, Yazawa M, Ueno T, Suzuki S, Yagi K. J Biochem (Tokyo) 1989;106:778–783. [PubMed: 2613684]
25. Wang CLA, Wang LWC, Lu RC. Biochem Biophys Res Commun 1989;162:746–752. [PubMed: 2757638]
26. Katayama E, Horiuchi KY, Chacko S. Biochem Biophys Res Commun 1989;160:1316–1322. [PubMed: 2525036]
27. Wang CLA, Carlos A, Lu RC. Biophys J 1990;57:162a.
28. Velaz L, Ingraham RH, Chalovich JM. J Biol Chem 1990;265:2929–2934. [PubMed: 2137453]
29. Wang CLA. Biochem Biophys Res Commun 1988;156:1033–1038. [PubMed: 3190671]
30. Lynch W, Bretscher A. Methods Enzymol 1986;134:37–42. [PubMed: 3821568]
31. Graceffa P, Wang CLA, Stafford WF. J Biol Chem 1988;263:14196–14202. [PubMed: 3170543]
32. Kuntz ID, Kauzman W. Adv Protein Chem 1974;28:239–345. [PubMed: 4598824]
33. Greenfield N, Fasman GD. Biochemistry 1969;8:4108–4116. [PubMed: 5346390]
34. King L, Lehrer SS. Biochemistry 1989;28:3498–3502. [PubMed: 2663071]
35. Graceffa P. Biochemistry 1989;28:1282–1287. [PubMed: 2713364]
36. Bailey, J. E. (1966) Ph. D. thesis, London University
37. Mabuchi K. J Struct Biol 1990;103:249–256. [PubMed: 2261309]
38. Bryan J. J Muscle Res Cell Motil 1989;10:95–96. [PubMed: 2668328]
39. Graceffa P, Jancso A. J Muscle Res Cell Motil 1990;11:440.
40. Graceffa P, Jancso A. Biophys J 1990;57:161.(abstr.)
41. Pearlstone JR, Smillie LB. Can J Biochem 1977;55:1032–1038. [PubMed: 562229]
42. Stafford WF III. Biochemistry 1985;24:3314–3321. [PubMed: 4027243]
43. Garcia de la Torre J, Bloomfield VA. Q Rev Biophys 1981;14:81–139. [PubMed: 7025081]
44. Herzberg O, James MNG. Nature 1985;313:653–659. [PubMed: 3974698]

45. Sundaralingam M, Bergstrom R, Strasberg G, Rao ST, Roychowdhury P, Greaser M, Wang BC. Science 1985;227:945–948. [PubMed: 3969570]
46. Babu YS, Sack JS, Greenhough TH, Bugg CE, Means AR, Cook WJ. Nature 1985;315:37–40. [PubMed: 3990807]
47. Yang DSC, Sax M, Chakrabartty A, Hew CL. Nature 1988;333:232–237. [PubMed: 3368002]
48. Maxfield FR, Scheraga HA. Macromolecules 1975;8:491–493. [PubMed: 1177494]
49. Marqusee S, Baldwin RL. Proc Natl Acad Sci U S A 1987;84:8898–8902. [PubMed: 3122208]
50. Sundaralingam M, Drendel W, Greaser M. Proc Natl Acad Sci U S A 1985;82:7944–7947. [PubMed: 3865207]
51. Sundaralingam M, Sekharudu YC, Yathindra N, Ravichandran V. Proteins Struct Funct Genet 1987;2:64–71. [PubMed: 3447168]
52. Marqusee, S., and Baldwin, R. L. (1990) in *Protein Folding: Deciphering the Second Half of the Genetic Code* (Gierasch, L. M., and King, J., eds) pp. 85–94, American Association for the Advancement of Science, Washington, D. C.
53. Shoemaker KR, Kim PS, York EJ, Stewart JM, Baldwin RL. Nature 1987;326:563. [PubMed: 3561498]
54. Åqvist J, Luecke H, Quiocho FA, Warshel A. Proc Natl Acad Sci U S A 1991;88:2026–2030. [PubMed: 2000410]
55. Hemric ME, Chalovich JM. J Biol Chem 1990;265:19672–19678. [PubMed: 2246251]
56. Chou PY, Fasman GD. Adv Enzymol 1978;47:45–148. [PubMed: 364941]
57. Gibrat JF, Garnier J, Robson B. J Mol Biol 1987;198:425–443. [PubMed: 3430614]
58. Garnier J, Osguthorpe DJ, Robson B. J Mol Biol 1978;120:97–120. [PubMed: 642007]

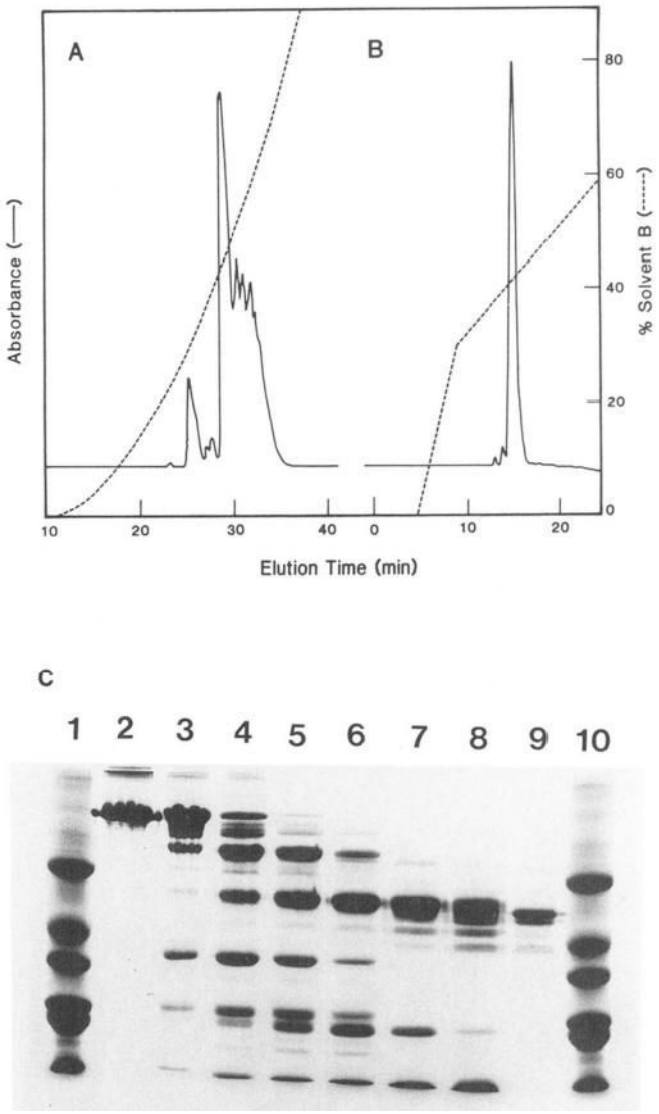

Fig. 1. The 54-kDa fragment of caldesmon obtained from chymotryptic digestion.

To purify CT54, the chymotrypsin digestion mixture (weight ratio of chymotrypsin to caldesmon = 1:700; t = 10 min) was chromatographed on a Waters HPLC using a Pharmacia Mono Q column with an exponential gradient to 500 mm NaCl (*A*). The major peak was concentrated and chromatographed on the same column using a linear gradient of NaCl from 185 to 500 mm (*B*). *C,* the time course of chymotrypsin digestion of caldesmon. *Lanes 1* and *10*, molecular mass standards (66, 45, 36, 29, 24, and 20.4 kDa); *lane 2*, caldesmon alone; *lanes 3–8*, caldesmon (2.6 mg/ml) treated with chymotrypsin (1:400 by weight), t = 0, 3, 6, 10, 30, 60 min, noting the transient appearance of the 40-kDa fragment and the relative stable bands around 54 kDa; *lane 9*, the HPLC-purified CT54.

Fig. 2. Determination of molecular weight of CT54 by sedimentation equilibrium measurements.
High speed equilibrium ultracentrifugation runs were performed as described previously (31). Plot shown are the number average molecular weight (M_n, *open circles*), the weight average molecular weight (M_r, *closed circles*), and the *z* average molecular weight (M_z, *open squares*) *versus* local cell concentration.

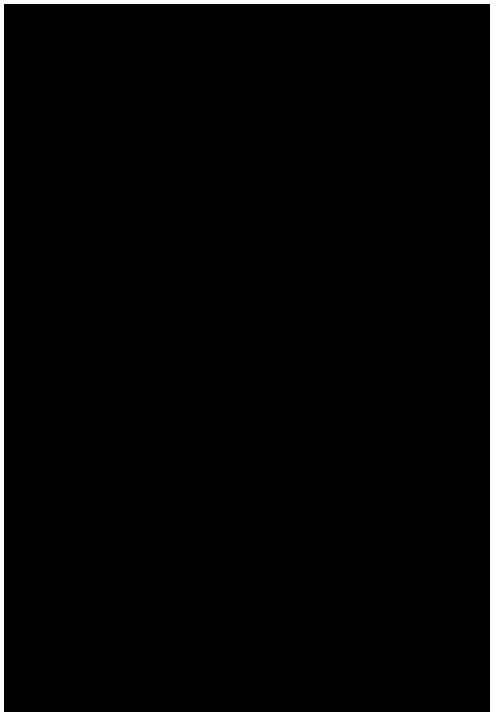

Fig. 3. Repeating sequence in the central region of smooth muscle caldesmon.
Shown here is the sequence in *one-letter code* from residues 166 to 450 with the repetitive units aligned in the middle. The sequence in *parenthesis* (*numbered 3′* and *underlined*) is the extra unit found in the longer isoform by Hayashi *et al*. (14). The residues in *italic* are variable parts in these repeats (see text for discussion). The leading unit (*numbered 0*) deviates significantly from the consensus sequence and may represent a degenerated motif. Alteration is also seen in the eighth unit which ends with an 11-residue insert.

Fig. 4. Secondary structures of gizzard caldesmon predicted by Chou-Fasman (56) (*A*) and Gibrat *et al*. (57) (*B*) algorithms.

The latter is a newer version of the Garnier-Osguthorpe-Bobson method (58). In the first method a string of 6 residues is considered, whereas in the second method, 17 residues are analyzed each time. The calculated conformational indeces (in arbitrary units) for α-helices (*solid lines*), β-sheets (*broken lines*), and random coils (*dotted lines*) are plotted. The beginning and the end of CT54 are indicated by *arrows*. Note that both methods predict that the central repeating region, residues from ~245 to ~400, has a high tendency to form α-helices, but a low tendency to form either β-sheets or random coils.

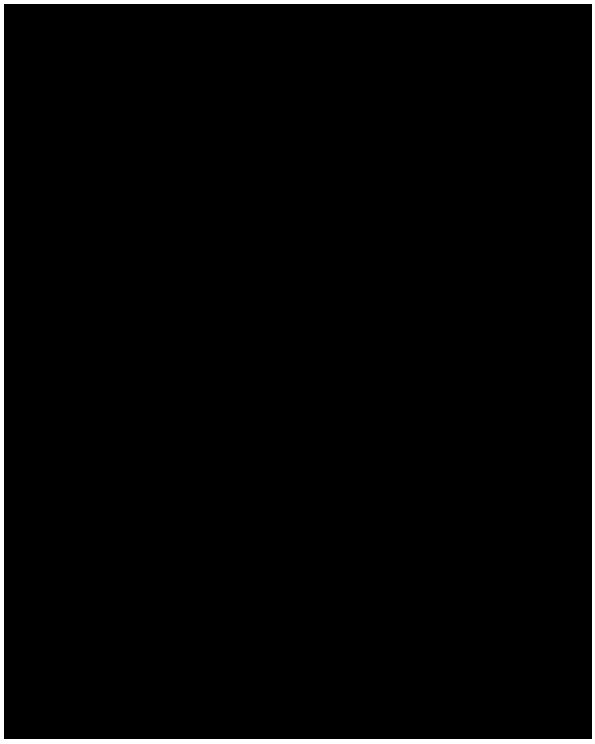

Fig. 5. Circular dichroism of CT54.

Panel A, CD spectra of CT54 in 2.5 mm potassium phosphate buffer, 0.04 mm EDTA, pH 7.6, 20 °C. *Panel B,* thermal unfolding measured at 222 nm of CT54 in 50 mm NaCl, 20 mm sodium phosphate buffer at pH 7.0 (*closed circles*), pH 2.02 (*open circles*), and pH 11.45 (*crosses*). At pH 9.5 the melting curve is identical to that at pH 7.0. Concentration of CT54, 0.047 mg/ml. All measurements were carried out in a 1-cm path length cell.

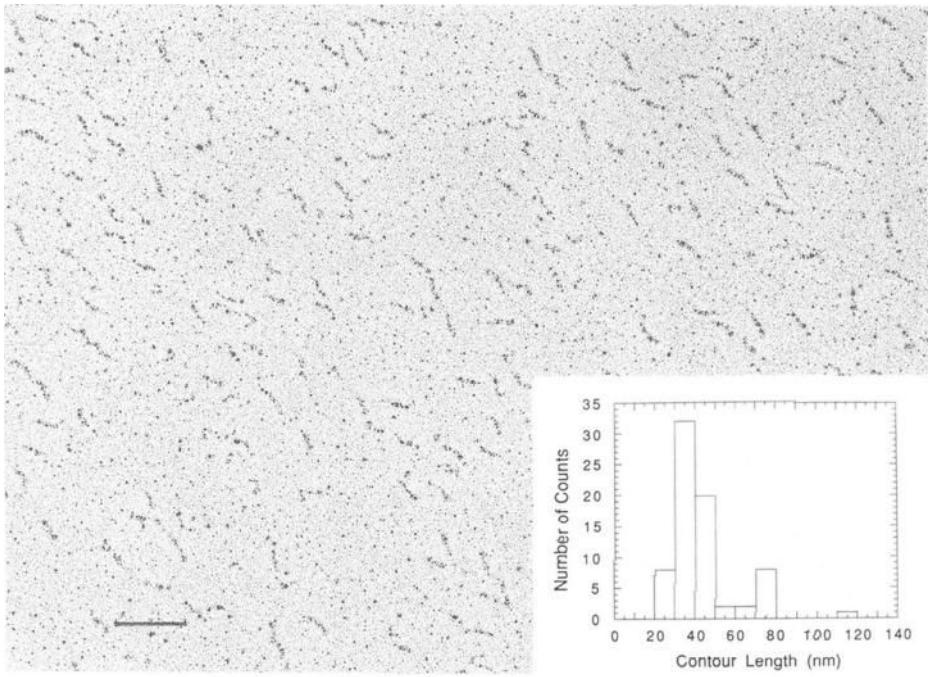

Fig. 6. Electron microscopic images of CT54.

CT54 (10–20 μg/ml) was sprayed onto the mica surface and processed for rotary shadowing by a platinum-rich mixture (platinum/tungsten = 3:1); *bar* indicates 100 nm; magnification, ×150.000. *Inset*, a typical histogram shows the distribution of the contour length of the images. The observed longer images are consistent with end-to-end oligomers.

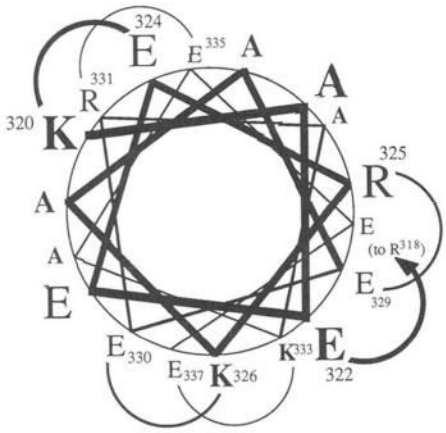

Fig. 7. Postulated salt bridges that may be responsible for stabilizing the helical structure of CT54.
Peptide segment from Lys^{320} to Glu^{337} is plotted in a helical wheel. Salt bridges are indicated by *curved lines*. Residues involved in salt bridge formation are labeled with *numbers*. Note that all salt bridges are formed between residues at positions *i* and *i*+4: Lys^{320} to Glu^{324}, Arg^{325} to Glu^{329}, Lys^{326} to Glu^{330}, etc. Glu^{322} is to interact with Arg^{318} which is not shown. Similar charge interactions are thought to operate in other repeating units (see Fig. 3).

Table I

Results of amino acid composition analysis of CT54 fragment

Amino acid	Observed	Calculated[a]
	%	%
Ala	15.34	16.1
Asx	6.55	6.67
Glx	33.5	33.7
Gly	1.65	1.05
His	<0.01	0
Ile	0.61	0.35
Lys	20.0	19.65
Leu	3.53	3.51
Met	0.76	1.05
Pro	1.99	1.75
Arg	7.56	7.37
Ser	1.87	2.1
Thr	3.08	2.46
Val	3.56	3.51
Tyr	<0.01	0
Trp		0.70

[a]Based on the sequence from Gln^{166} to Trp^{450} (13).

Table II

Comparison of calculated helical content of caldesmon fragments

Protein/fragment	Residues	α-Helical%	Method of determination	No. of residues involved in α-helices
Gizzard caldesmon	1–756	~40[a]	$[\theta]_{208\ nm}$	302
Liver caldesmon	1–524	31[b]	$[\theta]_{208\ nm}$	162
Difference peptide	200–432	60	Calculated	140
CT54	166–450	55[c]	$[\theta]_{208\ nm}$	157
		58[c]	Curve fitting[d]	165

[a] Ref. 40.

[b] P. Graceffa, and A. Jancso, unpublished results.

[c] This work.

[d] Obtained by curve fitting of the entire CD spectrum of CT54 to basis spectra (33).